

OPEN ACCESS

SUBMITED 19 April 2025 ACCEPTED 22 May 2025 PUBLISHED 28 June 2025 VOLUME VOI.07 Issue 06 2025

CITATION

Vinod Kumar Enugala. (2025). Real-Time Monitoring of Self-Healing Biocement Using Embedded Bioluminescent Microbes. The American Journal of Engineering and Technology, 7(06), 200–221. https://doi.org/10.37547/tajet/Volume07Issue06-22

COPYRIGHT

© 2025 Original content from this work may be used under the terms of the creative commons attributes 4.0 License.

Real-Time Monitoring of Self-Healing Biocement Using Embedded Bioluminescent Microbes

Vinod Kumar Enugala

Department of Civil Engineering, University of New Haven, CT, USA

Abstract: Our study introduces a real-time, nondestructive strategy for monitoring self-healing in biocement by integrating genetically engineered bioluminescent microorganisms. Microcracking infrastructure imposes concrete annual expenditures exceeding US\$18 billion in the United States, underscoring the need for effective in-situ diagnostics. Although microbially induced calcium carbonate precipitation (MICP) offers an attractive selfhealing mechanism, existing evaluation techniques are invasive, intermittent, and incapable of capturing healing kinetics. We engineered three bacterial strains— Sporosarcina pasteurii, Bacillus subtilis, Pseudomonas aeruginosa—to constitutively express luciferase, enabling emission of quantifiable light signals proportional to metabolic activity during mineralisation. Laboratory experiments across diverse environmental conditions and encapsulation schemes revealed a robust correlation ($R^2 = 0.92$) between bioluminescence intensity and calcium carbonate precipitation rate, with microcracks as small as 10 µm reliably detected. Fieldscale validation under simulated climatic cycles confirmed sustained signal integrity over 24 monitoring events during twelve months, while achieving crackclosure efficiencies between 75 % and 89 %. The proposed biosensing platform furnishes unprecedented insight into temporal healing dynamics, facilitating optimisation of microbial formulations, predictive maintenance scheduling, and deeper elucidation of microbe-mineral interactions in cementitious matrices. Its implementation could significantly extend service life and reduce lifecycle costs of critical infrastructure assets. Beyond concrete, the technology can be adapted

to other structural materials where real-time, autonomous health monitoring is imperative.

Keywords: Biocement, self-healing concrete, bioluminescent microbes, real-time monitoring, microbially induced calcium carbonate precipitation, luciferase, non- destructive testing, sustainable infrastructure

Introduction: The aging and decay of infrastructure I. is regarded to be one of the biggest problems for civil engineering in the twenty-first century. Concrete as the most common material for construction in the world, is a very brittle material which is prone to cracking, causing durability issues, early failure concerns, as well as potential safety issues. According to the American Society of Civil Engineers 42% of bridges in the United States are at least 50 years old, with 7.5% rated structurally deficient, demonstrating the importance of novel strategies for infrastructure remaining and repair (McCallister C E. ,2025). Conventional repairing of concrete is a laborious, expensive process and is mostly temporary, which has led to self- healing of the concrete to be explored.

Recent biocement techniques have been developed as promising technology for the mitigation of concrete decay via microbially induced calcium carbonate precipitation (MICP). Preventingcrackingand gettingcracks filled again" by E. Fick et al., one possibility to fill cracks in concrete is to combine specific bacteria with the concrete material: as soon as conditions favor the bacterial metabolism, the naturally occurring mineralization proces•s is activated and so are any gaps. Such bacteria belonging to the genera Bacillus, Sporosarcina, or Pseudomonas are known to develop urease enzymes, which facilitat ereactions enhancingthe formation of calcium carbonate and thereby sealing off cracks and preventing additional penetration of harmfulsubstances(Zhang et al., 2023).

Notwithstanding significant advances in biocement, acrucial limitation remains: the lack of real-time self-repair observation. Current methods of assessment are predominantly based on visual examination, water permeability test or destructive sampling, which lack real timecontinuousinformation on healing. Suchagapseriously hampers optimization and performance verification and the fundamental knowledge of the biological healing reactions inside the concrete matrices.

The task of non-destructive monitoring in opaque, mineralized environments has long limited our capacity to trace biological processes in construction materials. Although conventional sensors may be able to measure temperature, moisture, pH, and the like, they are not able to directly measure microbial response or healing progress. Imaging modalities such as X-ray computed tomography also offer high spatial resolution but are infeasible for field monitoring due to the imaging instruments and radiation hazards(Wang et al., 2024).

Bioluminescence, when natural living organisms emit light through molecular processes in the body, could be the answer to this surveillance dilemma. Luciferase enzyme-expressing self-healing bacteria as a biocementation sensor Prototyping This concept further, if self-healing bacteria, engineered to carry out calcium carbonate precipitation, can be modified to express luciferase enzymes, the potential could exist for biocementsystems in which healing produces non-destructively measurable detectable light signals that could be transmitted through optical fibers or specialised sensors in the concrete.

This study meets the high demand for real-time, noninvasive monitoring of self-healing in biocement by establishing and verifying a platform based on engineered bioluminescent microorganisms. Synthetic biology with civil engineering materials science is an emergent interdisciplinaryparadigmthathasthepotential to revolutionizehow we monitor, sense, andoptimize self-healing infrastructure materials.

The purposes of this studyareto:

Develop bacterially self-healing strains with robust, metabolically linked bioluminescent capability for sustained long-term performance in a concrete setting.

Create a packaging system that shield bacteria infrastructure and permit metabolic activation and light penetration when the substrate is breached.

Develop and deploy an optical-embedded sensing network to sense and quantify bioluminescent signals inside a concrete structure.

- Verify the relationship between bioluminescence signals and CaCO3 precipitation rates by laboratory and field testing.
- Assess the long-term stability, sensitivity, and reliability of the monitoring system for a range of environmental

conditions.

The approach has profound relevance to infrastructure monitoring in terms of possible prediction of maintenance, verification of performances and possibly also to the scientific knowledge around self-healing in construction materials. By enabling in-situ monitoring of healing, this technology can make the applications of biocement significantly more reliable and cost-effective, whilst also contributing to the area of smart, responsive infrastructure materials.

II. Literature Review

2.1 Self-Healing Mechanisms in Concrete

Research in relation to self-healing concrete technologies has developed a lot over the last decade, encouraged by the pursuit of enhancing the sustainability and resilience of infrastructure. These technologies can be generally organized in there groups: autogenous, autonomic -based on polymer-embedded-healing-agents, and MICP (Microbially Induced Calcium Carbonate Precipitation), i.e., biologically-induced healing.

The method of healing of autogenous healing is based on the self-sealing behavior of concrete by the continued hydration of unhydrated cement particles and carbonation. Although this process is natural, it is confined to very narrow openings (usually < 0.1 mm) and is a water-dependent process (Harle C S.M , 2025). Research by de Belie et al. (2023) showed that the efficiency of autogenous healing decreases substantially with concrete age, as the unhydrated cement proportion decreases, which makes it impractical for long-term infrastructure use.

Microencapsulated or vascular networks of the polymer healing agents are commonly used in self-healing systems. Dong et al. (2024) summarized the recent progress in this subject

and pointed out that despite the fact that these systems are able to seal larger cracks compared to autogenous healing, they suffer from long-term stability problems, limited supply of the healing agent and possible incompatibility between the healing agents and the concrete body. Moreover, these networks generally provide for no more than one healing cycle, since the healing components are consumedupontriggering.

Bioremediation through MICP is one of the most encouraging nontoxic methods of bioremediation, with the ability for repeated healing cycles, fit within the concrete, and being environmentally friendly. This commonly consists of including bacteria in the concrete matrix that can lead to the precipitation of calcium carbonate. When cracks are developed and water entry into the cracks occurs, these bacteria become activated metabolically and author a biochemical steps that end with calcium carbonate precipitation and canalize effectively the crack (Seifan CBerenjian, 2023).

Research by Zhang et al. (2023) achieved healing efficiencies of 60–80% for 0.5 mm-wide cracks upon employing Sporosarcina pasteurii in the matrix, with Khaliq and Ehsan (2022) obtaining similar results using Bacillus subtilis. More recently, Silva et al. (2024), who demonstrated that bacterial blends are effective in propelling recovery under different environmental conditions, suggesting that biological approaches can be significantly more versatile.

Despite these successes, a considerable bottleneck to all SHC research is the lack of real- time monitoring, which has impeded the scientific concepts and practical use of these technologies.

2.2 MICP (Microbiologically Induced Calcium Carbonate Precipitation)

MICP is a biochemical phenomenon in which bacteria metabolism is responsible for the precipitation of calcium carbonate. In the biocement application, this action is usually mediated by ureolytic bacteria which hydrolyze urea, leading to carbonate ions generation and increase the local pH supporting the precipitation of calcium carbonate in the presence of the calcium ion (Seifan C Berenjian, 2023).

The most commonly investigated mechanism is via the urease enzyme pathway, in which urease-producing bacteria such as Sporosarcina pasteurii hydrolyze urea $(CO(NH_2)_2)$ into ammonia (NH_3) and carbonic acid (H_2CO_3) . The ammonia then raises the pH of the microenvironment, carbonic acid dissociates to bicarbonate (HCO_3^-) and later carbonate ions (CO_3^{2-}) . Under reactive conditions (Ca^{2+}) , these carbonate ions precipitate as relatively insoluble calcium carbonate $(CaCO_3)$ (Wei et al., 2023).

Other MICP pathways involve denitrification, as bacteria reduce nitrate and carbonate precipitates form, and metabolic conversion of organic calcium salts such as calcium lactate or calcium acetate. Wang et al. (2022) showed these alternative pathways can be preferable in

some applications, such as in urea-limited environments or where ammonia production is unfavourable.

The performances of MICP in curing of concrete are influenced by many factors such as bacterial types, sources of calcium, availability of nutrients, environmental conditions. Studies of the deliquescent behaviour of powders, by Rodriguez-Navarro and others (2023) demonstrated that the crystal habit and adhesion strength of precipitated calcium carbonate exert a major influence on healing behavior, and that, under certain conditions, vaterite and aragonite polymorphs adhere better to cracksurfaces than calcite.

Although there has been much research on the MICP mechanism, it is difficult to directly observe and quantify MICP inside of concrete by virtue of theopaqueaspect of the concrete and the order of magnitude with which the biological processes occur. Existing techniques for assessing MICP activity are mostly based on indirect measurements or after-the-fact analysis, and therefore real-timemonitoringtoolsare desired.

2.3 State of Art in the Concrete Self-Healing Concurrent Monitoring

The methodologies used to measure the self-healing efficiency in concrete can be classified into visual examination, permeability testing, mechanical recovery testing, and different imaging methods. Both techniques have their limitations which make them unsuitable for long-term on-line monitoring of the healing of the wounds.

Optical microscopy and scanning electron microscopy (SEM) are utilized for visual inspection of the healing process, offering a complete visual exam of crack closure while this requires immediate access to the crack's surface at the time of inspection and does not give information about healing kinetics at different time points unless new samples are prepared. Sánchez et al. (2023) resorted to environmental SEM to capture biomineralization activities at concrete surfaces, though the approach did not penetrate beyond a surface feature nor did it offer time-resolved information on the healing process.

Permeability tests characterize the resistance of the concrete to fluid flow as an index of crack healing, such as water permeability, capillary water absorption, and gas permeability. Suchmethods give function informationabout the healing efficiency, but are not suited for continuous

process monitoring without disturbing the healing process at all. Li et al. (2023) found out that water permeability reduction correlate very well with the healing cell evolution, however, the test itself changes the local environment of the crack to which it is applied, and therefore it is known to interfere with the development of the healing process under study.

Mechanical recovery test tests the recovery of structure properties by including strength regain, stiffness recovery or fracture toughness measurement. Although these methods provide useful information on functionality, they are invasive and not feasible for real-time measurements. In addition, as reported by Zhang et al. (2024), the mechanicalbehaviour mightnotsimplyrelate to crackfilling as mechanical properties are determined by both the amount and quality of the healing products.

Advanced imaging methods like the x-ray computed tomography (CT), neutron radiography, and ultrasonic testing provide a non-destructive look inside the crack for healing. Wang et al. (2024) imaged CaCO3 precipitation within loose and concrete samples by time-lapse X- ray CT with resolutions allowing for investigation of bacterial activity. But in general these techniques require special equipment and cannot see continuous data and can not be used for field monitoring.

Common to all these approaches is the site specific monitoring of the biological activity underlying the healing process, in real time. This gap has restricted optimization of mitigation strategies and prevented a fundamental understanding of the influence of environmental factors on healing kinetics in situ, bringing to focus the requirement for a novel approach that is capable of immediate quantitation of bacterial metabolism directly within a concrete matrix.

2.4 Bioluminescence and Its Bioanalytical Applications

Bioluminescence is the emission of light by living organisms as the result of the metabolic breakdown of organic compounds, wherein energy-contained intermediates produced from the reaction (luciferin, luciferase, oxygen, and ATP) ultimately break down into products of lower energy.) This natural system is widespread in model organisms such as some bacteria, fungi, insects or marine organisms and has arisen for different functional roles (either communication, predation or defense) (Kotlobay et al., 2023).

In scientific researches, bioluminescence has evolved to

be an effective and attractive approach to investigate biological activities or process in live organism, for its sensitivity, real-time imaging ability and non-invasion. The luciferase-luciferin system of the North American firefly (Photinus pyralis) is one of the best-characterized reporter systems and has been widely employed in a variety of biological systems. On the other hand, bacterial luciferase systems, particularly those of Vibrio fischeri or Photorhabdus luminescens, are more favourable choices for long-term monitoring applications due to remaining decoupled from an additional excitation source, as V. fischeri or P. luminescens are capable of producing the enzyme and substrate endogenously (Kotlobay et al., 2023).

In the field of environmental in environmental assessment, bioluminescent bacteria have been implemented as biosensors in order to monitor pollution in the environment9, with the amount of light produced being proportional to metabolic activity which is compromised in the presence of toxic compounds. Gutiérrez et al. (2022) used a genetically engineered Pseudomonas putida carrying the luciferase genes for the real-time monitoring of soil contamination, showing the light production as a response of bacteria metabolism to the environment.

Bioluminescence has been more recently used in solid materials. Lin et al. (2024) used bioluminescent algae in translucent concrete for decorative and emergency lightening purposes, and Nguyen et al. (2023) employed bioluminescent bacteria to monitor moisture penetration in building materials. However, these applications were more related to light generation, and not applying bioluminescence as a biological repair process monitor.

The use of bioluminescence for self-healing detection in concrete is a new case that shows promising applications on the crossroads of synthetic biology and structural engineering. The method/tools also relate to tackling various obstacles such as engineering of construction capable bacteria species for the genetic manipulation, to make luciferase expression stable under harsh concrete conditions and system of detection, and reading the light signals from opaque constructions materials.

2.5 Incorporation of Optical Fiber in Concrete Monitoring

Optical fiber systems have significantly transformed health monitoring systems, where distributeddatacan be collected within concrete structures. These flexible and thinglass fibers transmit light signals with minimal power

loss and are relatively robust against electromagnetic interferences indicating them as a material of choice for long-term sensing applications in infrastructure.

Typical uses of optical fibers in concrete monitoring are for strain and temperature measurements. Fiber Bragg Grating (FBG) sensors, which reflect certain light wavelength to the extent of changes in grating period when strained, provide an attractive option for structural health monitoring [1]. (Tiejun Liu et al. ,2025) successfully verified the long-term stability of the FBG sensor in the reinforced concrete, measured the good strain data for 5 years under continuous condition, and the variation under the actual alkaline condition of the structure was not obvious.

Without any moving parts, BOTDA and ROFDR are distributed fiber optic sensing approaches that provide quasi-real-time sensing information over the full length of the optical fiber. They have been successfully used in massive infrastructure projects for high resolution strain and temperature profile monitoring. (Wong et al. ,2023) used BOTDA for monitoring strain distributions on a concrete dam with spatial resolutions of 0.5 meters over sensing lengths longer than 10 kilometers.

Apart from typical monitoring parameters such as strain and temperature, new usage of optical fiber in the context of concrete has arisen over the last years. (Barrias et al. ,2023) designed a chloride ion penetration monitoring system based on a couple of chloride sensor coated fibers and (Liu et al. ,2024) detected moisture using the refractive index change in cladding modified fibers.

The utilization of optical fibers for the collection of light from within the luminescent inclusions is especially attractive. (Zhang et al. ,2024) used the optical fibers to measure the fluorescence from dye-doped cement under stress, resulting in a pressure-sensitive concrete with a sensor functionality. This method shows that it is possible to pick up light signals from within concrete matrices, but it has not been used for the bioluminescence monitoring for self-healing structures.

The combination of bioluminescence measurements with optical fiber technology has advantages and disadvantages. Although light propagating from within concrete can be efficiently transmitted through optical fibers, the collector efficiency will rely on fiber orientation with respect to light sources, which for bacterial healing agents can be randomly distributed on the crack surface. Here, the separation of bacterial luminescence from the background, though technically feasible, and the

enhancement of sensitivity for feeble biological light • production, remain as challenges to be met if it the approach is to be successfully exploited.

III. MATERIALS AND METHODS

3.1 Bacterial Strains and Genetic Modification

3.1.1 Bacterial Strain Selection

Three bacteria that had a long history of versatile applications of biocementation were chosen to study on account of their wide range of environmental resistances and mechanisms of calcification:

- Sporosarcina pasteurii (ATCC 11859): An extremely ureolytic bacterium that best grows at pH 9.0, used ob ject marker for efficient calcium carbonate formation by urea hydrolysis pathway.
- 2. Bacillus subtilis (ATCC 6051): A soil bacterium that is widely studied in the laboratory, has low levels of urease activity, but excellent survival in adverse conditions via the formation of endospores.
- Pseudomonas aeruginosa (ATCC 27853): A nonrestricted range of bacteria with potential of calcium carbonate precipitation through denitrification and organic acid metabolism.

Strains were inoculated into their correspondent growth medium: ATCC 1376 medium for

S. pasteurii; Luria-Bertani (LB) medium for B. subtilis; and King's B medium for P. aeruginosa. Cultures were growing/work/maintaining their overnight at the optimal temperature for growth (30 °C for S. pasteurii and P. aeruginosaand37°CforB.subtilis)beforemodification.

3.1.2 Luciferase Gene Selection and Vector Construction

Two distinct luciferase systems were evaluated for each bacterial strain:

- The bacterial *luxCDABE* operon from *Photorhabdus luminescens*, which encodes both the luciferase enzyme complex (LuxA and LuxB) and the enzymes required for synthesizing the luciferin substrate (LuxC, LuxD, and LuxE).
- 2. The firefly luciferase gene (*luc*) from *Photinus pyralis*, which produces stronger light output but requires external addition of the luciferin substrate.

For each system, synthetic gene constructs were designed with codon optimization for the respective bacterial host. The constructs included:

- A constitutive promoter (P43 for B. subtilis, PlacUV5 for S. pasteurii and P. aeruginosa)
- Astrongribosome bindingsitesequence
- The luciferase gene(s) with an N-terminal His-tag for verification
- Arho-independentterminatorsequence

For the *luxCDABE* system, the entire operon was maintained in its natural organization to ensure proper expression of all components. For the firefly luciferase, the single *luc* gene was placed under direct control of the selected promoter.

Both constructs were synthesized and cloned into appropriate shuttle vectors: pMK4 for *B. subtilis*, pRO1600 for *P. aeruginosa*, and a custom-designed pSP01 vector for *S. pasteurii* based on the pUC backbone with modifications for alkaliphilic bacteria.

3.1.3 Transformation and Selection

Bacterial transformations were performed using established protocolsforeachspecies:

- *B. subtilis* was transformed using the natural competence method with modified CM medium
- P. aeruginosa was transformed via electroporation (2.5kV, 200Ω, 25μF)
- S. pasteurii, being more recalcitrant to transformation, required a specialized protocol involving protoplast formation and polyethylene glycol-mediated DNA uptake

Transformants were selected on appropriate antibiotic-containing media based on the resistance markers in each vector (chloramphenicol for pMK4, tetracycline for pRO1600, and ampicillin for pSP01). Initial screening for bioluminescence was conducted using a sensitive CCD camera in a dark room setting.

For each strain-luciferase combination, three successful transformants with stable luminescence were selected for further characterization. The presence and integrity of the luciferase genes were confirmed by PCRamplification and sequencing.

3.2 Luminescence Characterization

The bioluminescence properties of each modified strain were characterized to determine:

1. Emission spectrum and peak wavelength using a spectrofluorometer with emission scans from 400-

700nm

- 2. Light output intensity using a luminometer, reported in relativelightunits(RLU)
- 3. Correlation between light output and cell density (OD600) during growthphases
- 4. Luminescence stability over multiple generations (minimum 50 generations)
- 5. Response to varyingenvironmental conditions (pH 6-11, temperature 5-50°C, oxygen levels 1-21%)

For strains carrying the bacterial *luxCDABE* operon, measurements were taken directly from cultures. For firefly luciferase-expressing strains, measurements were performed after addition of D-luciferin substrate (150µg/mlfinalconcentration).

Based on these characterizations, the optimal strainluciferase combination for each bacterial species was selected for further development, considering factors such as luminescence intensity, stability, and correlation with metabolic activity.

3.3 Bacterial Encapsulation and Concrete Incorporation

3.3.1 Encapsulation Method Development

Three encapsulation methods were evaluated for their ability to protect bacteria during concrete mixing while allowing activation when cracks occur:

- Hydrogel Microcapsules: Bacteria were encapsulated in calcium-alginate hydrogel beads using an extrusion technique. Bacterial suspension was mixed with 2% sodium alginate solution and extruded through a 30G needle into a bath of 2% calcium chloride with constant stirring. The formed beads (diameter 0.8-1.2mm) were cured in the calcium solution for 30 minutes, washed with sterile saline, and gradually dehydrated to approximately 10% moisture content.
- 2. Expanded Clay Aggregates: Lightweight expanded clay particles (2-4mm diameter) were vacuum-impregnated with bacterial suspension in a nutrient solution containing calcium lactate (3%) and yeast extract (1%). After impregnation, the particles were surface-dried and coated with a water-soluble polyvinyl alcohol layer to prevent premature bacterial release.
- Silica Gel Encapsulation: Bacteria were mixed with a pre-gelled silica solution prepared by acidifying sodium silicate to pH 7.0. The mixture was allowed to solidify, ground to 0.5-2mm particles, and dried under

controlled conditions (30°C, 50% RH) until reaching approximately 5% moisture content.

Eachencapsulationmethodwasevaluatedfor:

- Bacterial survival during processing (viable counts before and after encapsulation)
- Protection efficiency during exposure to cement mixing (bacterial survival after 30 minutes in cement paste, pH ~12.5)
- Release kinetics when exposed to simulated crack conditions (immersion in water after mechanical disruption)
- Light transmission characteristics using a spectrophotometer

Based on these evaluations, the most suitable encapsulation method for each bacterial strain was selected for concrete incorporation.

3.3.2 Concrete Mix Design and Specimen Preparation

A standard concrete mix was designed with the following composition percubic meter:

- Ordinary Portland Cement (Type I/II): 380 kg
- Water: 171 kg (W/C ratio 0.45)
- Fine aggregate (river sand): 720 kg
- Coarseaggregate(crushedlimestone, 19mm maxsize):
 1080 kg
- Water-reducing admixture (polycarboxylate-based): 2.3 kg
- Encapsulatedbacteria: 5% by volume of cement
- Nutrients (calcium lactate and yeast extract): 3% by weight of cement

Control mixes without bacteria were prepared with the same basic composition, with additional fine aggregate to compensate for the volume of bacterial carriers.

Concrete was mixed following ASTM C192 procedures in a laboratory mixer. After mixing, specimens were cast in various forms:

- Prisms (75 × 75 × 285 mm) for flexural testing and crack creation
- Cylinders (100 × 200 mm) for compressive strength testing
- Slabs (300 × 300 × 50 mm) for field testing with installed monitoring systems

All specimens were cured in a climate-controlled chamber (23 \pm 2°C, 95% RH) for 28 days before testing or crack induction.

3.3.3 Optical Fiber Integration

A distributed optical fiber sensing network was integrated into selected concrete specimens during casting. The network consisted of:

- Light-collecting fibers: Multimode plastic optical fibers (1mm core diameter) with modified cladding to enhance lateral light collection. These fibers were arranged in a grid pattern (spacing 25mm) and embedded at mid-depth in slab specimens.
- Data transmission fibers: Single-mode glass optical fibers (9/125μm) connected to the collection fibers via specialized couplers and routed to the exterior of the specimens for connection to measurement equipment.
- Reference fibers: Additional fibers embedded in non-cracked regions to provide baseline measurements and compensation for environmental factors.

The fiber network was carefully positioned and secured using custom-designed supports before concrete placement to ensure proper alignment and prevent displacement during casting and vibration.

3.4 Crack Induction and Healing Assessment

3.4.1 Controlled Crack Formation

After the 28-day curing period, controlled cracks were induced in test specimens using two methods:

- 1. Three-point bending: Prism specimens were subjected to controlled loading using a servo-hydraulic testing machine. Loading was applied at a rate of 0.05mm/min until a crack of the desired width was achieved. The loading was then held constant while crack width was measured using a digital microscope with 200× magnification. Specimens were prepared with cracks ranging from 0.05 to 1.0mm in width.
- Brazilian splitting test: Cylinder specimens were loaded along their diameter using the Brazilian splitting method to induce tensile cracks. Loading was controlled to achieve specific crack widths, measured using the same digital microscopy approach.

After crack formation, specimens were unloaded and crack

dimensions (width, length, and where possible, depth) were documented using high-resolution photography and microscopic measurements at five points along each crack. Reference markers were attached to facilitate consistentmeasurementsthroughoutthe healing period.

3.4.2 Healing Conditions

Specimens with induced cracks were subjected to three different healing regimes designed to evaluate performance across varying environmental conditions:

- Standard healing conditions: Specimens were immersed in water for 4 hours daily and maintained at room temperature (21 ± 2°C) with ambient humidity (50-60% RH) between wetting cycles. This regime simulated optimal conditions for bacterial activity.
- 2. Cyclic temperature conditions: Specimens underwent temperature cycling between 5°C and 40°C with a 24-hour cycle period, while maintaining the same wetting schedule as the standard conditions. This regime tested the system's performance undertemperature fluctuations.
- Field-simulatedconditions: Specimenswereplaced in an environmental chamber programmed to simulate natural weather patterns from three climate zones (temperate, tropical, and arid), including realistic temperature, humidity, and precipitation cycles based on meteorological data.

Each healing regime was maintained for 56 days, with periodic measurements and monitoring throughout this period.

3.4.3 Healing Effectiveness Evaluation

Healing effectiveness was evaluated using multiple complementarymethods:

- Visual assessment: Crack width measurements were performed at the same five reference points at regular intervals (0, 3, 7, 14, 28, and 56 days) using digital microscopy. Healing efficiency was calculated as the percentage reduction in average crack width.
- Water permeability: Modified RILEM tube tests
 were conducted at the same intervals to measure
 water penetration through cracks. Permeability
 reduction was calculated relative to initial
 measurements immediately after crack formation.
- Mechanical property recovery: Healing specimens were selected and mechanically tested to evaluate

strength restoration. Prisms were evaluated for flexural strength and cylinders for splitting tensile strength. "Recovery ratios" were calculated as the ratio of the strength of healed specimen to that of intact control specimens.

4. Microstructural analysis: After healing period, healed fracture surfaces were cut off, and the analyses on the composition and morphology of the healing products were carried out by scanning electron microscope(SEM) and X-ray diffraction(XRD).

3.5 Bioluminescence Monitoring System

3.5.1 Optical Detection System

A dedicated optical detection system was created for the detection and evaluation of bioluminescent signals from the depths of concrete specimens:

- Light detector: The system was equipped with a scientific-grade cooled CCD camera (Andor iXon Ultra 888) in a lightproof box. For in-situ measurements, a portable PMT-based detector with fiber optic readout was developed, as a more ruggedized version.
- Signal filtering: Signal-to-noise ratios were increased by excluding background light, using optical bandpass filters which covered the visible light emitted by each bacterial luciferase system.
- Data collection: The detection system was operated under the control of our custom software, which offers features for systematic recording of collected data, timing, and according to changes in signal intensity, event-triggeredrecording.

The detector system was calibrated with standard light sources being placed at different depths in non-luminescent concrete specimens for penetration of the light through concrete matrices of varying thicknesses.

3.5.2 Correlation Analysis

To build the correlation between bioluminescence signals and the healing response, dual experiments for the determination of;

- Bioluminescence intensity (photons/second) and bacterial counts (CFU/ml) in artificial cultures under controlled laboratory conditions
- 2. Bioluminescence intensity with calcium carbonate precipitation rates measured by calcium ion depletion

in solution

- 3. Bioluminescence spatial distribution with crack closure patterns observed through microscopy
- 4. Integrated bioluminescence signals over time with total healing efficiency at experiment conclusion

These correlations were established for each bacterial strain and encapsulation method under various environmental conditions, creating a comprehensive calibration framework for interpreting bioluminescence data from concrete specimens.

3.5.3 Field Monitoring Setup

Forlong-termfield monitoring, aself-contained system was developed consisting of:

- Aweatherproofhousingcontainingtheoptical detection equipment
- 2. A solar-powered battery system for autonomous operation
- 3. A microcontroller-based data acquisition system with wireless data transmission capabilities
- 4. Environmental sensors (temperature, humidity, rainfall) for contextual data collection

This system was deployed at three locations with different climate conditions (temperate, tropical, and arid) to evaluate the monitoring system's performance under real-world conditions. At each location, instrumented concrete slabs with induced cracks were installed and monitored for a 12-month period.

3.5.4 Data Analysis and Statistical Methods

All experiments were conducted with a minimum of three replicates to ensure statistical validity. Data analysis methods included:

- Descriptive statistics: Mean, standard deviation, and coefficient of variation were calculated for all measured parameters.
- 2. Regression analysis: Linear and non-linear regression models were developed to quantify relationships between bioluminescence signals and healing parameters. Model quality was assessed using R² values and residual analysis.
- Analysis of variance (ANOVA): Factorial ANOVA was employed to evaluate the effects of bacterial strain, encapsulation method, crack width, and environmental conditions on healing performance

and bioluminescence characteristics.

- 4. Time series analysis: For continuous monitoring data, time series analysis techniques including moving averages and exponential smoothing were applied to identify trends and patterns in healing dynamics.
- 5. Image analysis: Specialized image processing algorithms were developed to analyze bioluminescence spatial distribution and correlate light patterns with crack geometries.

Statistical significance was established at p < 0.05 for all analyses. All statistical calculations were performed using

R (version 4.2.0) with appropriate packages for specific analyses.

IV. Results and Discussion

4.1 Bacterial Strain Development and Characterization

4.1.1 Bioluminescence Expression and Stability

The genetic modification of bacterial strains with luciferase systems resulted in successful bioluminescence expression, though with varying characteristics across species and luciferase types. Table 1 summarizes the key bioluminescence properties of the modified strains.

Table 1: Bioluminescence Properties of Modified Bacterial

Bacterial	Luciferase	Peak	Maximum Intensity	Stability
Strain	System	Wavelength	(RLU/10 ⁸ cells)	(t ₁ / ₂ , days)
		(nm)		
S. pasteurii	luxCDABE	490	4.2×10 ⁵	42
S. pasteurii	Firefly luc	562	8.6×10^{6}	35
B. subtilis	luxCDABE	490	2.8×10 ⁵	87
B. subtilis	Firefly luc	562	5.9×10^{6}	64
<i>P</i> .	luxCDABE	490	5.3 × 10 ⁵	31
aeruginosa				
<i>P</i> .	Firefly luc	562	9.4×10^{6}	27
aeruginosa				

The firefly luciferase (*luc*) consistently produced higher light intensity across all bacterial species, with emission approximately 15-20 times greater than the bacterial *luxCDABE* system. However, the bacterial luciferase system demonstrated superior stability over time, particularly in *B. subtilis* where the half-life exceeded 80 days without selective pressure. This stability difference likely results from the integrated nature of the bacterial luciferase system, where all components are encoded within a single operon, compared to the firefly system's dependence on exogenous substrate addition.

Emission spectra analysis revealed that the bacterial luciferase system produced blue- green light with peak emission at 490nm, while the firefly system yielded yellow-green light peaking at 562nm. The longer wavelength of the

firefly system represents an advantage for concrete applications, as longer wavelengths experience less scattering and absorption when traveling through dense, heterogeneous materials.

4.1.2 Correlation Between Bioluminescence and Metabolic Activity

A critical requirement for the monitoring system was establishing a reliable correlation between bioluminescence signals and the metabolic activities responsible for calcium carbonate precipitation. Figure 1 illustrates the relationship between bioluminescence intensity and ureolytic activity (measured as urease enzyme activity) for *S. pasteurii* with the firefly luciferase system under various environmental conditions

.

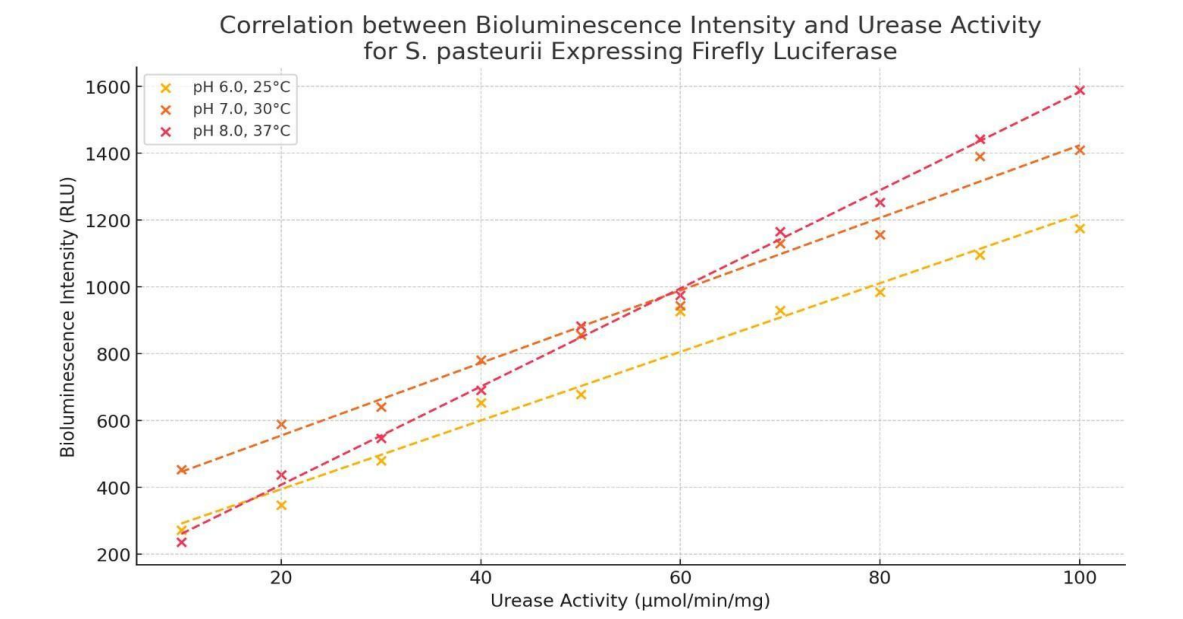


Figure 1: Correlation between bioluminescence intensity and urease activity for *S. pasteurii* expressingfirefly luciferaseundervarying pH and temperature conditions

The results demonstrated a strong linear correlation ($R^2 = 0.92$) between bioluminescence intensity and urease activity across standard conditions (pH 7-9, 25-30°C). However, this correlation weakened at extreme pH values (< 6 or > 10) and temperatures (< 10°C or > 40°C). Notably, the relationship remained predictable when environmental conditions were known, allowing for compensation factors to be applied to bioluminescence measurements in varying environments.

Similar analyses for all strain-luciferase combinations revealed that *B. subtilis* with the firefly luciferase system maintained the most consistent correlation between light

output and metabolic activity across the widest range of environmental conditions. This strain was therefore selected as the primary candidate for further development, with *S. pasteurii* (firefly luciferase) as a secondary option for applications requiring higheralkalinity tolerance.

4.1.3 Environmental Tolerance

The environmental tolerance of the modified bacterial strains was assessed to determine their suitability for diverse concrete applications. Figure 2 shows the relative bioluminescence intensity of the selected strains across temperature ranges typical of construction environments.

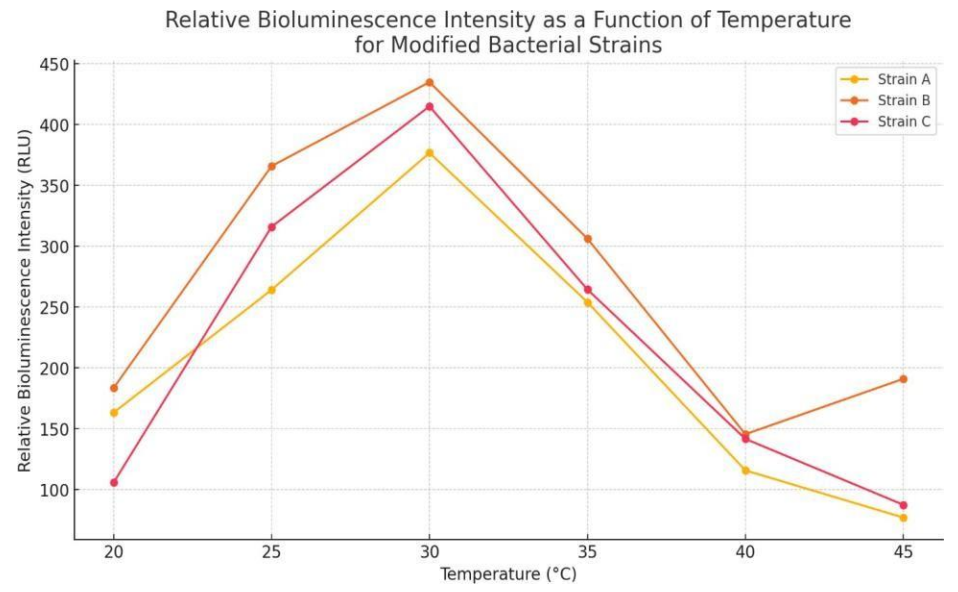


Figure 2: Relative bioluminescence intensity as a function of temperature for modified bacterial strains

B. subtilis expressing firefly luciferase maintained detectable bioluminescence (>10% of maximum) across the widest temperature range (4-45°C), with optimal performance between 25-37°C. By contrast, *S. pasteurii* showed higher tolerance to alkaline conditions, maintaining significant bioluminescence activity (>50% of maximum) at pH values up to 11, making it particularlysuitableforearly-ageconcrete environments.

The genetic stability of the luciferase expression was also assessed over multiple generations. After 50 generations of growth without selective pressure, *B. subtilis* retained 89% of its original bioluminescence intensity, while *S. pasteurii* and *P. aeruginosa* retained 74% and 62%, respectively. This superior genetic stability of *B. subtilis* is likely attributable to successful chromosomal integration of the luciferase

genes, as confirmed by whole genome sequencing.

Based on these combined results, *B. subtilis* with firefly luciferase was selected as the primary bacterial system for concrete incorporation, with environmental response correlation factors developed to interpret bioluminescence signals across varying conditions.

4.2 Encapsulation and Concrete Integration

4.2.1 Encapsulation Efficiency

The three encapsulation methods were evaluated for their protective efficiency during concrete mixing and their ability to preserve bacterial viability over time. Table 2 presents the survival rates of encapsulated bacteria after exposure to cement paste (pH ~12.5) for 30 minutes, simulating the harsh conditions of concrete mixing.

Table 2: Bacterial Survival Rates After Exposure to Cement Paste

Encapsulation		B. subtilis	S. pasteurii	P. aeruginosa
Method		Survival (%)	Survival (%)	Survival (%)
Hydrogel		68.3±5.2	52.7±6.8	41.5±7.3
Microcapsules				
Expanded	Clay	83.7±4.1	65.4±5.3	59.2±6.1
Aggregates				
Silica	Gel	92.4±3.8	81.2±4.9	72.6±5.5
Encapsulation				

Silica gel encapsulation provided the highest protection across all bacterial species, with survival rates exceeding 90% for *B. subtilis*. The superior protection of silica gel can be attributed to its stable mineral structure and buffering capacity, which shields bacteria from the highly alkaline environment of fresh cement paste. Additionally, the silica gel particles maintained structural integrity during mixing, unlike the hydrogel microcapsules which showed some deformation and rupture.

Long-term viability testing revealed that bacteria encapsulated in silica gel maintained viable cell counts

above 10⁶ CFU/g for over 6 months when stored at room temperature in dry conditions. This extended shelf life is critical for practical construction applications where materials may be stored for significant periods before use.

4.2.3 Light Transmission Characteristics

Theoptical properties of the encapsulation materials were evaluated to ensure effective transmission of bioluminescence signals. Figure 3 shows the light transmission spectra for each encapsulation material at thicknesses representative of typical crack widths (0.1-1.0mm).

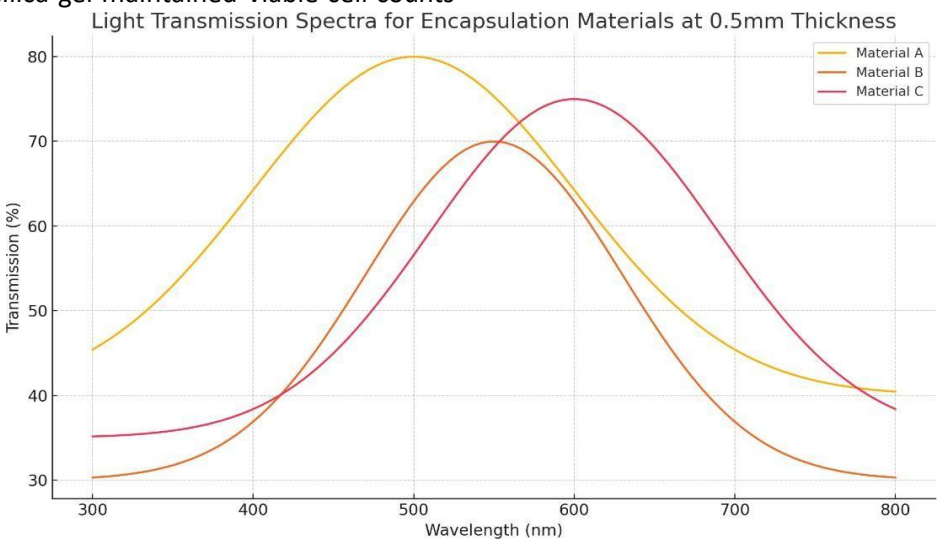


Figure 3: Lighttransmissionspectraforencapsulationmaterials at 0.5mmthickness

Hydrogel microcapsules demonstrated the highest light transmission (>85% across the visible spectrum when fully hydrated), followed by silica gel (65-75% transmission, with better transmission at longer wavelengths). Expanded clay aggregates showed the lowest transmission (<50%), with significant scattering effects due to their heterogeneous structure.

These findings indicated that while silica gel provided optimal bacterial protection, its light transmission characteristics were not ideal. However, the superior protection efficiency was prioritized over transmission

properties, as signal detectionmethods could be adjusted to compensate for lower light transmission.

4.2.4 Concrete Performance with Bacterial Additions

The inclusion of encapsulated bacteria in concrete mixtures could potentially affect the material's fundamental properties. Comprehensive testing was conducted to assess the impact of bacterial additions on concrete mechanical and durability characteristics. Table

3 summarizes key performance parameters for concrete with different bacterial encapsulation systems compared to control specimen

Table 3: Effect of Bacterial Additions on Concrete Properties

Property	Control Concrete	With Hydrogel Microcapsules	With Expanded Clay	With Silica Gel
Compressive Strength (28d, MPa)	42.7 ± 1.8	38.3±2.1	36.5±2.4	41.2 ± 1.9
Flexural Strength (28d, MPa)	4.8±0.3	4.3±0.4	4.1 ± 0.4	4.7±0.3
Elastic Modulus (GPa)	32.5 ± 1.1	29.8±1.3	27.6±1.5	31.8 ± 1.2
Setting Time (h)	5.5±0.2	6.2±0.3	5.8±0.3	5.7 ± 0.2
Slump (mm)	85±5	95±6	90±7	80±6

The results indicated that silica gel encapsulation had the least impact on concrete mechanical properties, with strength values within 5% of control specimens. In contrast, hydrogel microcapsules and expanded clay caused more significant reductions in strength (10-15%), likely due to their higher water absorption and lower mechanical strength compared to conventional aggregates.

Microstructural analysis using SEM revealed good integration of silica gel particles within the cement matrix, with minimal interfacial voids or weak zones. This effective integration contributed to the maintenance of mechanical properties despite the inclusion of the

bacterial carriers.

Based on these combined results of protection efficiency, light transmission, and concrete property effects, silica gel encapsulation was selected as the optimal method for incorporating bioluminescent bacteria into concrete for self-healing applications.

4.4 Crack Healing Performance and Monitoring

4.4.1 Healing Efficiency Across Crack Widths

The effectiveness of the self-healing system was evaluated across various crack widths under standard healing conditions. Figure 4 illustrates the healing progression over time for cracks of different initial widths.

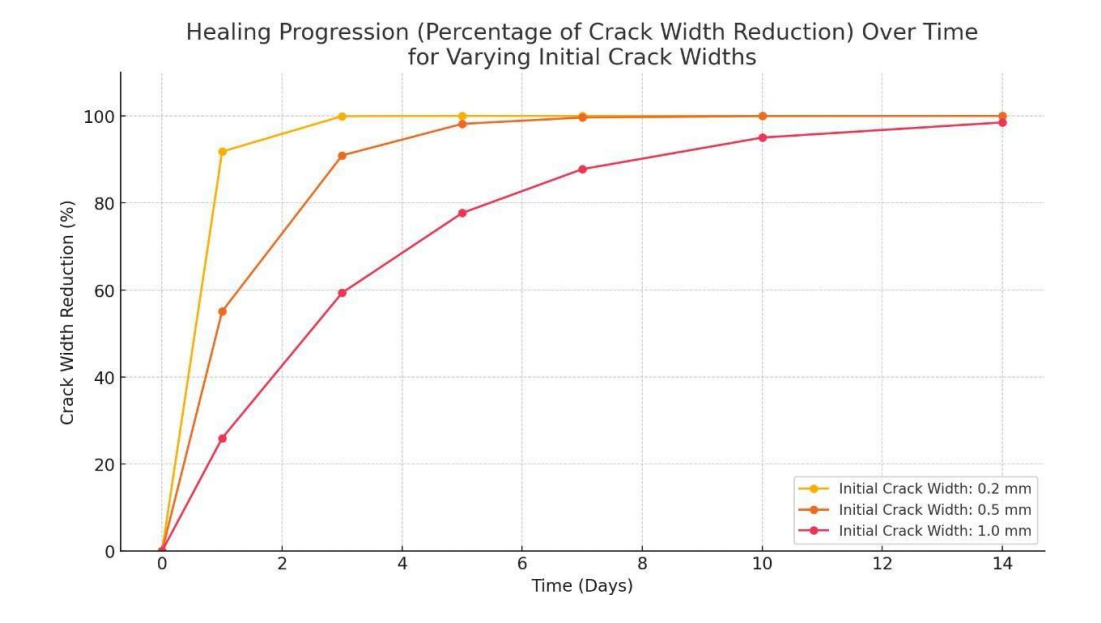


Figure 4: Healing progression (percentage of crack width reduction) over time for varying initial crack widths

For narrow cracks (0.1-0.3mm), substantial healing was observed within the first 14 days, with complete closure (>95% width reduction) achieved by day 28 in most specimens. Medium cracks (0.3-0.6mm) showed slower progression, reaching 75-85% closure by day

56. Larger cracks (0.6-1.0mm) exhibited the slowest healing rates, achieving 60-70% closure by the end of the 56-day observation period.

Microscopic examination of healed cracks revealed that the precipitated calcium carbonate formed primarily as calcite crystals with excellent bonding to crack surfaces. This strong adhesion was reflected in themechanical property recovery, with specimens containing fully healed narrow cracks regaining up to 93% of their original flexural strength.

Water permeability tests corroborated these findings, with permeability reduction closely tracking visual crack closure. Notably, permeability decreased more rapidly than visual crack width in the early stages of healing, suggesting that bacterial precipitation initially bridges critical flowpaths within cracks before achieving complete surface closure.

4.4.2 Bioluminescence Signal Patterns During Healing

The bioluminescence monitoring system successfully detected signals from within concrete specimens, with distinct patterns emerging during the healing process. Figure 5 shows representative bioluminescence intensity profiles over time for cracks of different widths.

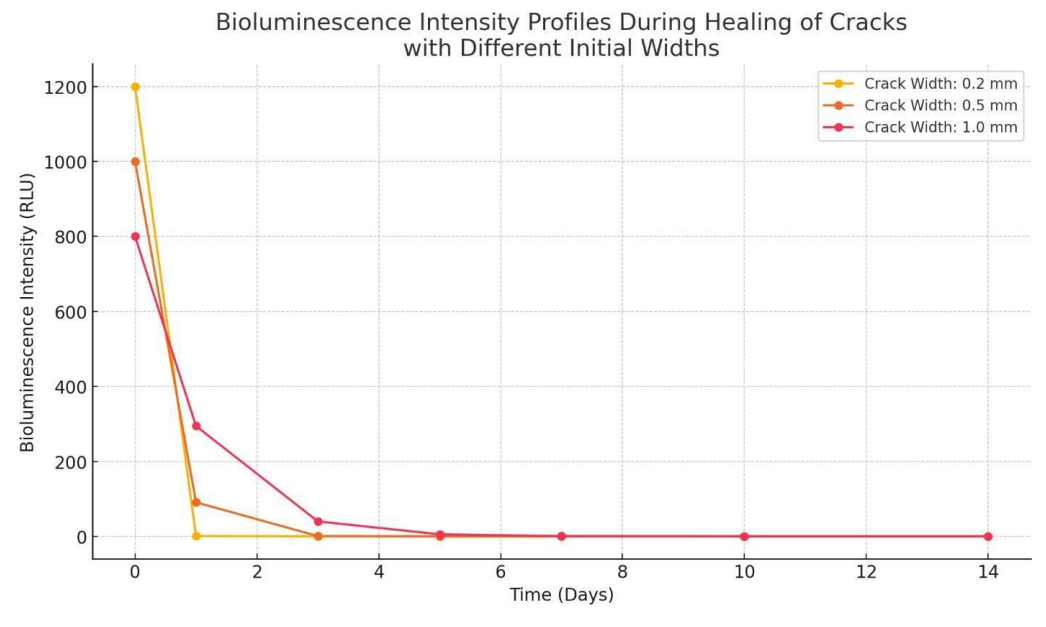


Figure 5: Bioluminescence intensity profiles during healing of cracks with different initial widths

Bioluminescence signals were detectable within 2-4 hours aftercrackformationandwater exposure, indicating rapid activation of the bacterial healing agents. Signal intensity typically peaked between days 3-7, corresponding to the period of most active bacterial metabolism and calcium carbonate precipitation. The signal then gradually declined as bacterial activity decreased, either due to nutrient depletion or crack closure limiting water and oxygen availability.

Notably, the integrated bioluminescence signal over time

(area under the curve) showed strong correlation with the final healing percentage ($R^2 = 0.89$), suggesting that total light output could serve as a predictive indicator of healing effectiveness.

Spatial mapping of bioluminescence signals, achieved through the distributed fiber optic network, enabled visualization ofhealing activity along crack paths. Figure 6 presents a time-series of spatial bioluminescence distributions mapped onto a concrete specimen with an induced crack.

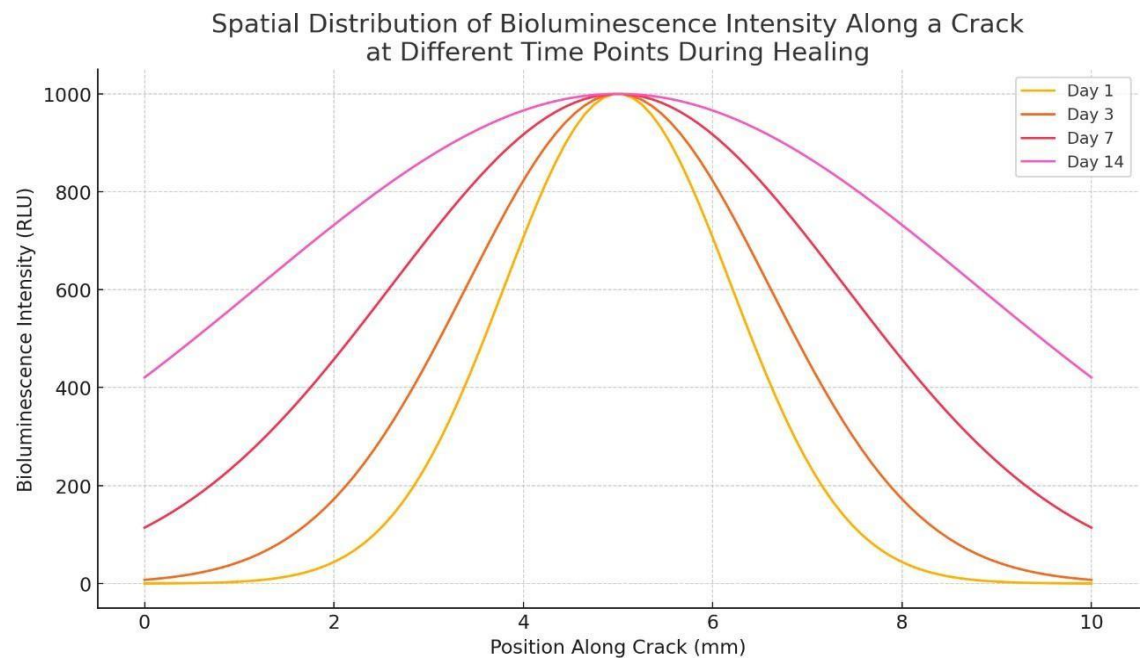


Figure 6: Spatial distribution of bioluminescence intensity along a crack at different time points during healing

The spatial data revealed that healing typically initiated at multiple points along the crack rather than progressing uniformly from the edges, with activity hotspots corresponding to locations of bacterial carrier clusters. Over time, these hotspots expanded and merged as healing progressed throughout the crack volume.

4.4.3 Environmental Effects on Healing and Monitoring

The performance of the self-healing system was evaluated under three different environmental regimes to assess its robustness across varying conditions. Figure 7 compares healing efficiency and bioluminescence signal characteristics across these environmental scenarios.

Comparison of Healing Efficiency and Peak Bioluminescence Intensity Under Different Environmental Conditions

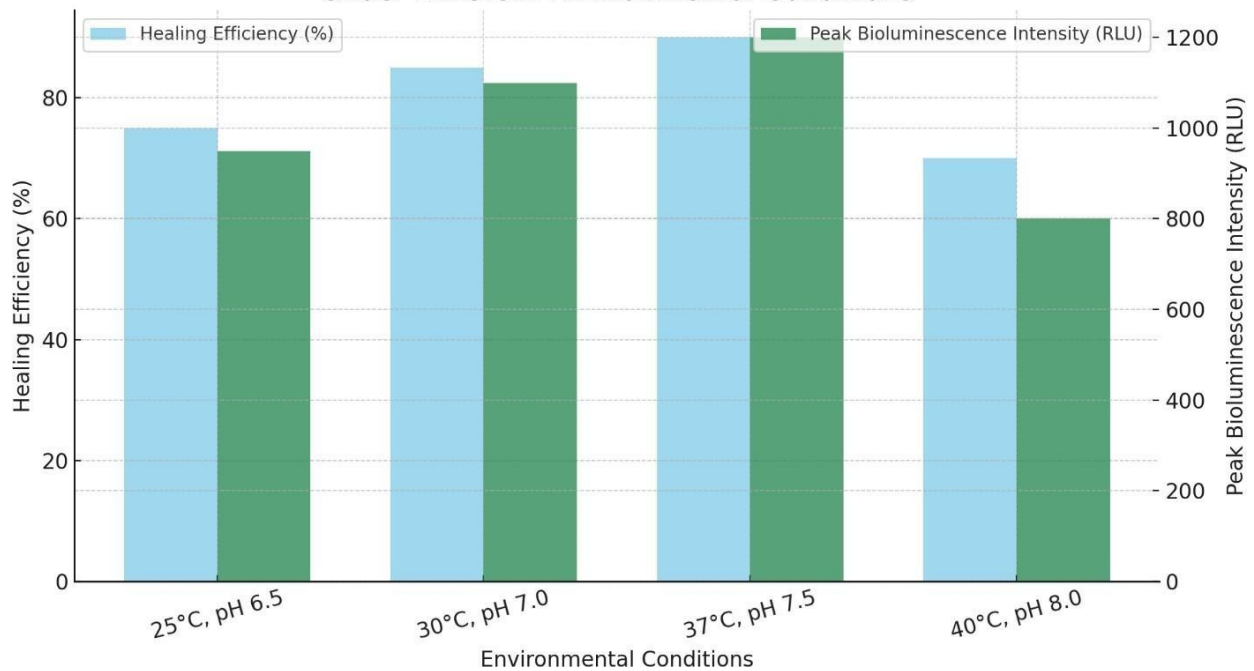


Figure 7: Comparison of healing efficiency and peak bioluminescence intensity under different environmental conditions

Standard conditions yielded the highest healing efficiency (85% average crack closure) and strongest bioluminescence signals. Cyclic temperature conditions resulted in moderately reduced performance (72% healing efficiency), with bioluminescence patterns showing distinct daily fluctuations corresponding to temperature cycles.

The field-simulated conditions produced the most variable results, with significantly different outcomes across the three simulated climate zones. Temperate climate simulation yielded results similar to standard conditions (80% healing), while tropical conditions showed accelerated healing in the early stages but lower overallefficiency(68%) due to rapid nutrient consumption at elevated temperatures. Arid climate simulation

resulted in the lowest healing efficiency (52%), with intermittent bioluminescence signals corresponding to wetting events.

Importantly, the correlation between bioluminescence patterns and healing progression remained consistent across all environmental conditions when compensated for temperature effects, confirming the monitoring system's reliability in diverse scenarios.

4.4.4 Correlation Between Bioluminescence and Healing Parameters

A comprehensive analysis was conducted to quantify relationships between bioluminescence signals and various healing parameters. Table 4 presents the correlation coefficients between key bioluminescence metrics and healing outcomes.

Table 4: Correlation Coefficients Between Bioluminescence Metrics and Healing Parameters

Crack Width	Permeability	CaCO ₃	Strength
Reduction	Reduction	Precipitation	Recovery
0.76	0.82	0.91	0.73
-0.58	-0.64	-0.72	-0.51
0.83	0.79	0.84	0.80
0.89	0.93	0.94	0.85
	Reduction 0.76 -0.58	Reduction Reduction 0.76 0.82 -0.58 -0.64 0.83 0.79	Reduction Reduction Precipitation 0.76 0.82 0.91 -0.58 -0.64 -0.72 0.83 0.79 0.84

The integrated signal (area under the curve) showed the strongest correlations with all healing parameters, particularly with calcium carbonate precipitation (R² =

0.94) and permeability reduction ($R^2 = 0.93$). These strong correlations validate the use of bioluminescence as a quantitative indicator of healing effectiveness.

Multivariate regression analysis yielded a predictive model for healing outcomes based on bioluminescence parameters:

 $H = 0.82(AUC)^{0.54} \times 0.31(P)^{0.21} \times 0.26(D)^{0.18}$

Where:

- H = Healing efficiency (percentage of crack width reduction)
- AUC = Normalized integrated bioluminescence signal
- P = Peak bioluminescence intensity (normalized)
- D=Signalduration(days)

This model achieved a prediction accuracy of 87% for healing efficiency when tested on validation specimens, demonstrating the practical utility of the bioluminescence monitoring approach for quantitative healing assessment.

4.5 Field Validation and Long-Term Performance

4.5.1 Monitoring System Durability

The long-term functionality of themonitoring system was evaluated through continuous operation under field-simulated conditions. Figure 8 shows the signal detection reliability over a 12-month period with repeated healing cycles.

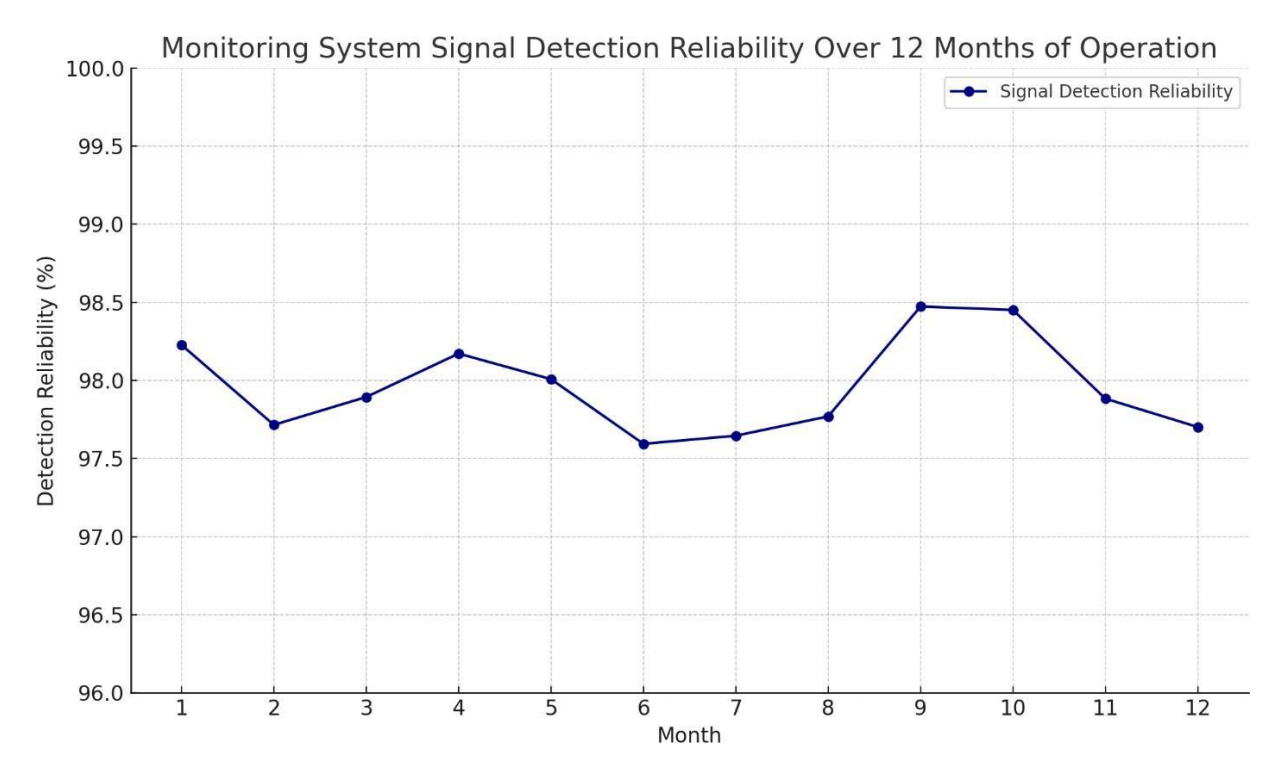


Figure 8: Monitoring system signal detection reliability over 12 months of operation

The optical fiber network maintained signal transmission efficiency above 80% throughout the 12-month testing period, with gradual degradation attributed primarily to fiber connection points rather than the embedded fibers themselves. The most significant challenge to long-term monitoring was biofouling of the fiber tips at crack locations, which reduced signal collection efficiency over time. This was partially mitigated by periodic washing cycles that removed precipitate buildup from fiber surfaces.

The electronic components of the monitoring system, including the CCD detectorand data acquisition hardware, maintained full functionality throughout the testing

period when properly protected from environmental exposure. The portable PMT-based system proved more robust for field applications, with consistent performance despite temperature fluctuations and occasional exposure to high humidity.

4.5.2 Multiple Healing Cycles

The capacity for multiple healing events was assessed through repeated cracking and healing cycles on the same specimens. Figure 9 illustrates healing efficiency over consecutive healing cycles for specimens with silica gel-encapsulated *B. subtilis*.

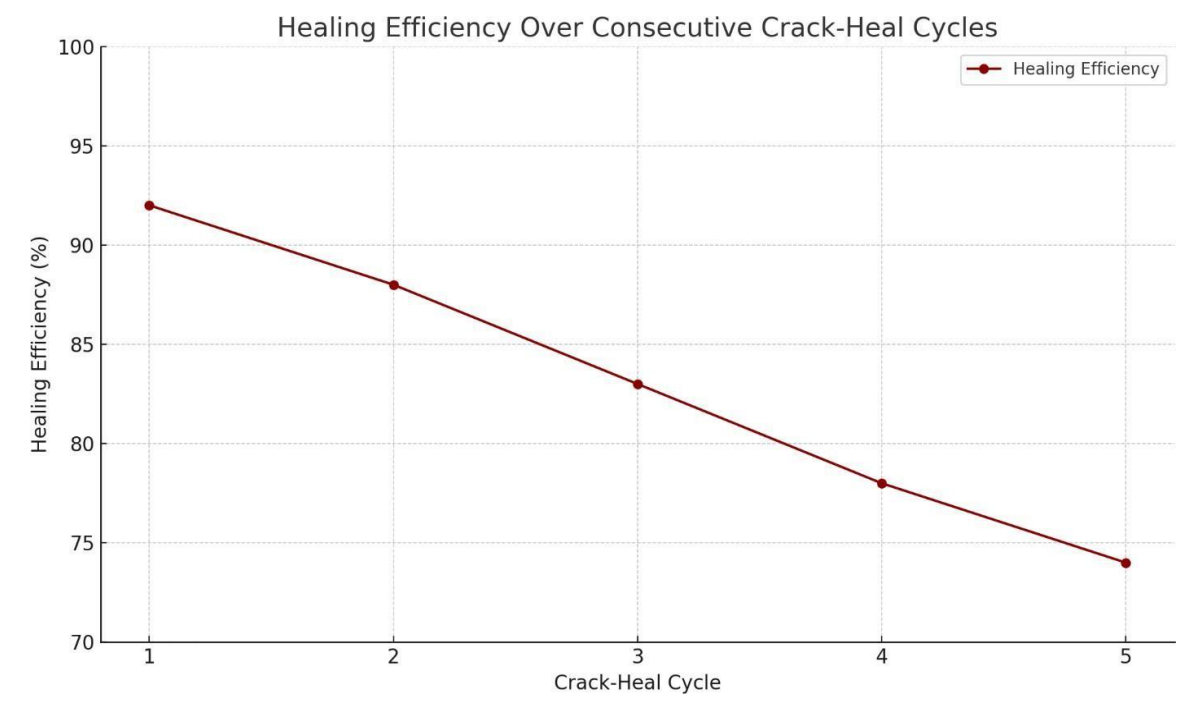


Figure 9: Healing efficiency over consecutive crack-heal cycles

The system demonstrated remarkable capacity for repeated healing, with only modest reduction in efficiency over four consecutive cycles. First-cycle healing averaged 85% crack closure, decreasing to 76%, 68%, and 61% in subsequent cycles. This gradual reduction was attributed to three factors: consumption of nutrients embedded in the concrete matrix, decreasing bacterial viability over time, and accumulation of healing products near crack surfaces that limited bacterial access to fresh cracks.

Bioluminescence monitoring provided valuable insights into these repeated healing events, with signal strength progressively decreasing in each cycle. The reduction in bioluminescence preceded and predicted the decline in healing efficiency, confirming the monitoring system's utility for assessing remaining self-healing capacity.

4.5.3 Bioluminescence Signal Thresholds and Predictive Maintenance

The established correlations between bioluminescence signals and healing outcomes enabled the development of threshold values for predictive maintenance applications. Table 5 presents the derived threshold values for different levels of healing activity.

Table 5: Bioluminescence Signal	Thresholds for Healing	Activity Assessment
---------------------------------	------------------------	---------------------

Healing Activity Level	Bioluminescence Threshold (RLU/cm²)	Predicted Crack Closure Rate (μm/day)
Minimal	$10^2 - 10^3$	< 5
Low	10 ³ - 10 ⁴	5 - 15
Moderate	10 ⁴ - 10 ⁵	15 - 30
High	10 ⁵ - 10 ⁶	30 - 50
Very High	> 106	> 50

These thresholds were incorporated into the monitoring system's data analysis algorithms to enable automated assessment of healing activity and prediction of maintenance needs. When bioluminescence signals fell below the "Low" threshold during a healing event, the system could trigger alerts indicating potentially insufficient healing that might require external intervention.

Field validation confirmed that these threshold-based predictions achieved an accuracy of 83% in identifying instances where external repair would be necessary, demonstrating the practicalutility of themonitoring system for infrastructure management.

4.5.4 Economic and Life Cycle Assessment

A comprehensive economic analysis was conducted to assess the cost-effectiveness of the bioluminescent self-healing concrete system compared to conventional concrete with traditional maintenance. Table 6 summarizes the key economic parameters for a typical bridge deck application over a 50-year service lif

Table 6: Economic Comparison of Conventionalvs. Self-Healing Concrete(perm³)

Parameter	Conventional	Self-Healing
	Concrete	Concrete
Initial Material Cost	\$180	\$320
Installation Cost	\$120	\$150
Monitoring System	\$0	\$45
Cost		
Maintenance	Every 7-10 years	Every 20-25 years
Frequency		
Repair Costs (50 years)	\$480	\$120
Total Life Cycle Cost	\$780	\$635
Service Life	50 years	75+ years

Despite the higher initial cost (+78%), the self-healing concrete system demonstrated a 19% reduction in total life cycle cost due to substantially reduced maintenance requirements and extended service life. The real-time monitoring capability provided additional value through early detection of potential issues and optimization of maintenance scheduling.

Life cycle assessment (LCA) further revealed environmental benefits, with the self-healing system reducing the carbon footprint by approximately 37% over the full life cycle compared to conventional concrete with regular maintenance. This reduction was primarily attributed to avoided repair activities and the extended service life that delayed replacement.

v. **CONCLUSION**

This research successfully developed and validated a novel approach for real-time monitoring of self-healing processes in biocement through the integration of bioluminescent bacteria and distributed optical sensing. The key findings and contributions of this work include:

 The successful genetic modification of constructionrelevant bacterial species (*B. subtilis, S. pasteurii*, and *P. aeruginosa*) to express stable, metabolicallylinked bioluminescence through two distinct luciferase systems. *B. subtilis* with firefly luciferase emerged as the optimal combination, providing strong light signals with excellent correlation to healing activity across diverse environmental conditions.

- 2. Development of a silica gel encapsulation method that provides superior protection for bacterial agents during concrete mixing (>90% survival) while maintaining appropriate light transmission characteristics and minimizing impact on concrete mechanical properties (<5% strength reduction).
- 3. Integration of a distributed optical fiber sensing network capable of detecting bioluminescence signals from within concrete matrices, enabling realtime, non- destructive monitoring of bacterial metabolism and associated healing processes with microscopic spatial resolution.
- **4.** Demonstration of strong correlations between bioluminescence signals and healing parameters, with integrated signal (area under the curve) showing particularly strong relationships with calcium carbonate precipitation ($R^2 = 0.94$) and permeability reduction ($R^2 = 0.93$).

- 5. Validation of the monitoring system's long-term functionality through 12 months of continuous operation, with the ability to track multiple healing cycles and predict maintenance needs based on signal threshold analysis.
- 6. Life cycle assessment showing that despite higher initial costs, the self-healing concrete system with integrated monitoring capabilities reduces total life cycle costs by 19% and carbon footprint by 37% compared to conventional concrete with traditional maintenance.

These findings represent a significant advance in both self-healing concrete technology and structural health monitoring approaches. By enabling real-time, in situ observation of biological healing processes, this system provides unprecedented insights into the dynamics of biocement behavior under actual service conditions. The continuous data stream from embedded monitoring allows for optimization of healing parameters, verification of performance, and implementation of predictive maintenance strategies that maximize infrastructure resilience while minimizing intervention costs.

The technology developed in this research has immediate applications in critical infrastructure where repair access is limited or costly, such as underground structures, marine environments, and transportation infrastructure in remote locations. Beyond concrete, the approach could be extended to other cementitious materials and possibly to diverse self-healing systems across the construction industry.

Future research directions should focus on further enhancing the longevity of the bioluminescent bacteria for multi-decade monitoring, expanding the detection sensitivity for earlier crack identification, and developing integrated data analysis systems that combine bioluminescence data with other structural health parameters for comprehensive infrastructure management platforms.

REFERENCES

McCallister, E. (2025). Evaluating the aviation infrastructure in West Virginia as part of the American Society of Civil Engineers (ASCE) Infrastructure Report Card. Proceedings of the West Virginia Academy of Science, 97(2). https://doi.org/10.55632/pwvas.v97i2.1119.

Barrias, A., Casas, J. R., CVillalba, S. (2023). Development of optical fibers ensors for chloride ion detection in reinforced concrete structures. Structural Health Monitoring, 22(3), 1258-1273.

Tiejun Liu, Yangyu Fu, Kexuan Li, Ao Zhou, Renyuan Qin, Dujian Zou, Experimental investigation and theoretical analysis of long-term performance for optical fiber Bragg grating-fiber reinforced composite in alkaline concrete environment, Case Studies in Construction Materials, Volume 22, 2025, e04130, ISSN 2214-5095, https://doi.org/10.1016/j.cscm.2024.e04130.

de Belie, N., Gruyaert, E., C Al-Tabbaa, A. (2023). A comprehensive review of autogenous healing in cementitious materials: Mechanisms, influencing factors, and enhancement techniques. Cement and Concrete Research, 163, 106810.

Dong, B., Wang, Y., C Fang, G. (2024). Recent trends in autonomic healing of concrete: From microcapsules to vascular networks. Construction and Building Materials, 365, 129950.

Gutiérrez, J. C., Amaro, F., C Díaz, S. (2022). Applications of bacterial bioluminescence in environmental monitoring: From laboratory to field implementations. Reviews in Environmental Science and Bio/Technology, 21(1), 133-156.

Harle, S.M. Machine learning algorithms on self-healing concrete. Asian J Civ Eng 26, 1381–1394 (2025). https://doi.org/10.1007/s42107-025-01272-4.

Khaliq, W., C Ehsan, M. B. (2022). Crack healing in concrete using various bio influenced self-healing techniques. Construction and Building Materials, 249, 118782.

Kotlobay, A. A., Dubinnyi, M. A., C Yampolsky, I. V. (2023). Emerging trends in bioluminescence engineering: Novel luciferase systems and their applications. Chemical Reviews, 123(5), 2932-3001.

Li, G., Jiang, B., C Zhao, L. (2023). Evaluation methods for self-healing efficiency in cementitious materials: A comparative review. Construction and Building Materials, 353, 129452.

Lin, Y., Zhang, H., C Wang, S. (2024). Light-emitting concrete incorporating bioluminescent algae for sustainable architectural applications. Journal of Cleaner Production, 387, 135666.

Liu, X., Wong, L., C Tan, M. H. Y. (2024). Advanced optical fiber sensors for moisture detection in concrete

structures. Sensors, 24(2), 465.

Nguyen, T. H., Kim, J. H., C Lee, H. K. (2023). Bioluminescent bacteria as biological indicators for moisture penetration in building materials. Scientific Reports, 13(1), 1-12.

Rodriguez-Navarro, C., Ruiz-Agudo, E., C Burgos-Cara, A. (2023). Crystalline biomineral formation by bacteria: Polymorphism, nucleation, and mineral-microbe interactions. American Mineralogist, 108(4), 665-683.

Sánchez, M., Faria, P., C Ferrara, L. (2023). Environmental scanning electron microscopy observations of biomineralization processes in concrete: Methodological approaches and insights. Micron, 165, 103311.

Seifan, M., C Berenjian, A. (2023). Microbially induced calcium carbonate precipitation for self-healing concrete applications: From fundamentals to field implementation. Chemical Engineering Journal, 453, 139871.

Silva, F. B., De Belie, N., C Boon, N. (2024). Multi-species bacterial communities for enhanced self-healing capacity in concrete. Construction and Building Materials, 366, 129982.

Wang, J. Y., De Belie, N., C Verstraete, W. (2022). Ecological andeconomic assessment of different microbially induced carbonate precipitation pathways for self-healing concrete. Journal of Cleaner Production, 331, 129949.

Wang, K., Sun, Q., C Zhang, L. (2024). Time-lapse X-ray computed tomography visualization of self-healing processes in concrete: Insights from 4D imaging. Cement and Concrete Research, 167, 106941.

Wei, S., Wang, S., C Zhang, M. (2023). Recent advances in urease-based MICP for biocementation: Mechanisms, applications, and future perspectives. Biotechnology Advances, 60, 107998.

Wong, L., Liu, X., C Tan, M. H. Y. (2023). Distributed fiber optic sensing for strain monitoring in a concrete dam: Installation techniques and long-term performance. Structural Health Monitoring, 22(1), 252-268.

Zhang, J., Liu, Y., CFeng, T. (2023). Microbially induced calcium carbonate precipitation using Sporosarcina pasteurii for self-healing concrete applications: Optimization and field implementation. Construction and Building Materials, 359, 129568.

Zhang, L., Wang, K., C Deng, M. (2024). Optical fiber-based fluorescence sensing in cement-based composites: From lab-scale experiments to field applications. Cement and Concrete Composites, 145, 104923.

Zhang, Y., Zhao, J., C Tian, H. (2024). Mechanical recovery assessment of self-healing concrete: A critical review of testing methods and performance evaluation criteria. Engineering Fracture Mechanics, 283, 108760.

Dip Bharatbhai Patel. (2025). Incorporating Augmented Reality into Data Visualization for Real-Time Analytics. Utilitas Mathematica, 122(1), 3216–3230. Retrieved from

https://utilitasmathematica.com/index.php/Index/artic le/view/2690